

¹⁹F Nuclear Magnetic Resonance as a Probe of Structural Transitions and Cooperative Interactions in Heavy Meromyosin*

(Received for publication, August 19, 1986)

Lewis E. Kay†, J. Michael Pascone, Brian D. Sykes§, and John W. Shriver¶||

From the ¶Department of Medical Biochemistry, School of Medicine, Southern Illinois University, Carbondale, Illinois 62901 and the §Medical Research Council Group on Protein Structure and Function, Department of Biochemistry, University of Alberta, Edmonton, Alberta, Canada T6G 2H7

An ¹⁹F NMR probe has been attached to the reactive sulphydryl SH₁ of the globular heads of rabbit skeletal heavy meromyosin. It serves as a sensitive monitor of the conformational state of the heads of heavy meromyosin in a manner similar to that seen for subfragment-1 (Shriner, J. W., and Sykes, B. D. (1982) *Biochemistry* 21, 3022-3028; Tollemar, U., Cunningham, K., and Shriner, J. W. (1986) *Biochim. Biophys. Acta* 873, 243-251). The NMR spectra indicate that there are at least two states for the heads in the SH₁ region. The energetics of the interconversion of the two states of heavy meromyosin (HMM) differs significantly from that of S-1. In HMM in the absence of divalent cations, there are two reversible paths between the low temperature and high temperature states with a hysteresis-like behavior. One path is consistent with the head groups behaving independently and similar to S-1 alone. The second path indicates a coupling of the globular head region observed in S-1 with a second region forming a distinctly different cooperative unit. Upon addition of Ca(II) the hysteresis effect is lost and only the second cooperative unit is observed. Two explanations are offered for these results: 1) the globular heads in HMM may couple with the S-2 segment, or 2) the two globular heads of HMM may couple to form a larger cooperative unit. The ability to stabilize the larger cooperative unit with a divalent metal ion implicates a role for the LC2 light chain in coupling regions of the myosin molecule.

We have recently demonstrated using ³¹P and ¹⁹F NMR that myosin subfragment-1 (S-1)¹ can exist in at least two discrete states with a highly temperature dependent equilib-

* This work has been supported by a National Institutes of Health New Investigator Research Award AM30712 (to J. W. S.), a grant from the Muscular Dystrophy Association of America (to J. W. S.), by the Alberta Heritage Foundation for Medical Research (Summer Fellowship to L. E. K.), and the Medical Research Council of Canada through a grant to the Medical Research Council Group on protein structure and function (to B. D. S.). The costs of publication of this article were defrayed in part by the payment of page charges. This article must therefore be hereby marked "advertisement" in accordance with 18 U.S.C. Section 1734 solely to indicate this fact.

† Present address: Dept. of Chemistry, Yale University, New Haven, CT 06520.

|| To whom correspondence should be addressed.

§ The abbreviations used are: S-1, myosin subfragment-1; SH₁, sulphydryl-1 of the myosin head; S-1-CF₃, subfragment-1 reacted with *N*-(4-trifluoromethylphenyl)iodoacetamide; HMM, heavy meromyosin; HMM-CF₃, heavy meromyosin reacted with *N*-(4-trifluoromethylphenyl)iodoacetamide; ATPase, adenosine triphosphatase; PIPES, 1,4-piperazinediethanesulfonic acid; DTNB, 5,5'-dithiobis-(2-nitrobenzoic acid).

rium constant (1-6). The relative population of the two states is controlled by the nucleotide in the active site, pH, and ionic strength. Interest in these two states has been stimulated by the possibility that they may be involved in energy transduction and may be correlated with pre- and post-power stroke states (4, 5).

Myosin is an oligomeric protein composed of six subunits: two heavy chains and four light chains (LC1, two copies of LC2, and LC3). Each of the heavy chains forms a globular S-1 head which contains an actin binding site and an ATPase active site. We are interested in mapping interactions between regions of myosin as part of a long-range goal of understanding energy transduction within myosin. The studies reported here have been performed with heavy meromyosin (HMM), a proteolytic derivative of myosin which retains the two-headed structure of myosin but is soluble at physiological ionic strength and appears to function in a manner identical to that of myosin (7). We have investigated the effect of Ca(II) and Mg(II) ions on the two-state transition in the structure of the two heads of HMM.

The release of Ca(II) by the sarcoplasmic reticulum plays a central role in excitation-contraction coupling. Striated muscles are regulated by the troponin-tropomyosin system through Ca(II) binding to troponin C (8-10). In addition Ca(II) activates a specific kinase which phosphorylates the DTNB light chain (11). In scallop, a regulatory light chain, resembling the LC2 light chain, confers Ca(II) sensitivity onto scallop myosin and links the two globular heads into a cooperative unit (12, 13). The rabbit LC2 light chain can restore Ca(II) sensitivity to desensitized scallop muscle (12) and this may indicate that the role of this polypeptide in striated rabbit muscle is not trivial (14). However the role of the LC2 light chain in vertebrate skeletal muscle has not been delineated. It has been argued that its affinity for Ca(II) is not selective enough to allow it to function as a rapid calcium-sensitive switch controlling the myosin ATPase (15, 16).

Using ¹⁹F NMR we show here that each of the two globular heads of heavy meromyosin, each of which contains an LC2 light chain, can exist in two discrete states in the region of SH₁. SH₁ is located in the 20-kDa fragment, which is adjacent to the hinge connected to S-2 (52). The structure of the two states in the vicinity of SH₁ appears to be identical to that observed for the isolated S-1 heads. The equilibrium between the two states is highly temperature-dependent in the range of 0-30 °C, allowing a study of the thermodynamics of the interconversion of the two states. Significant differences are seen between the energetics of interconversion of the two states of HMM when compared to S-1. These results imply that the cooperative unit in HMM may extend beyond the globular heads. A cooperative interaction between the heads

would also account for the data. Calcium ion, and magnesium ion, serve to stabilize the larger cooperative unit.

MATERIALS AND METHODS

α -Chymotrypsin was obtained from Cooper/Worthington. Special enzyme grade ammonium sulfate was obtained from Schwarz/Mann or Research Plus. D_2O was purchased from Bio-Rad and stored over Chelex 100 to ensure removal of trace paramagnetic ions. Ultra-pure PIPES and Tris were obtained from Behring Diagnostics. Dialysis tubing was obtained from Spectrum. All other chemicals used were of reagent grade. Laboratory distilled water was further purified by passage through Brinkman organic removal, high capacity mixed-bed and ultra-pure mixed bed cartridges, two 0.2- μ filter cartridges, and finally glass distilled. All solutions were stored in glass.

All procedures, unless otherwise indicated, were performed at or below 5 °C. All dialyses were performed in an ice-water slush at 1 °C. Sodium azide was used throughout at 0.1 mM to prevent bacterial growth. Myosin was isolated by standard procedures from rabbit back and leg muscle from freshly killed rabbits (1, 17, 18) and precipitated three times by dilution at 1 °C. HMM was prepared by digestion of myosin with 0.025 mg/ml chymotrypsin in 0.6 M NaCl, 0.01 M Na_2HPO_4 , 0.01 M Na_2HPO_4 , 0.02 M $MgCl_2$, pH 7.0 at 25 °C for 2 min (19). Digestion was terminated with phenylmethylsulfonyl fluoride (dissolved in a minimal volume of spectrograde acetonitrile) to give a final concentration of 0.5 mM. The temperature was quickly lowered to 1 °C.

HMM was purified by chromatography on either DEAE-cellulose (Whatman DE-52) or DEAE-trisacryl M (LKB Instruments, Inc.). Protein fragments were eluted with a linear gradient of NaCl (0–0.5 M NaCl in 50 mM Tris, 2.5 mM $MgCl_2$, pH 7.9).

The purity of HMM preparations was checked by sodium dodecyl sulfate gel electrophoresis which indicated the presence of LC2 light chain at a level equal to the sum of the alkali light chains (see Fig. 1). The light chain ratios in HMM were also compared to that of fresh myosin. In addition, the purity of the HMM preparations and also the presence of aggregation were monitored with native gel electrophoresis using 5% acrylamide gels.

ATPase activities were determined by using a Radiometer pH stat. Ca^{2+} ATPase activity of the modified protein was measured in 0.6 M KCl, 10 mM $CaCl_2$, 5 mM ATP, pH 7.9 and 25 °C. A typical value was 5 s⁻¹. K^+ EDTA activity of the modified protein was measured in a solution of 0.6 M KCl, 5 mM EDTA, and 5 mM ATP at 25 °C and gave typically a result of 2.7 s⁻¹.

Purified HMM was labeled with a 4-fold molar excess (2-fold with respect to the number of heads) with the fluorine probe, *N*-(4-trifluoromethylphenyl)iodoacetamide, by the method described pre-

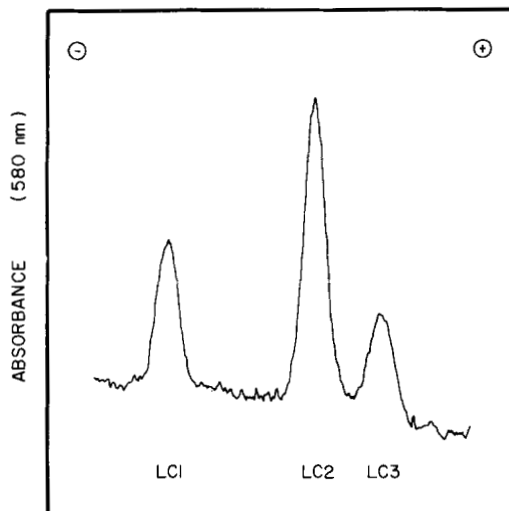


FIG. 1. A densitometric scan at 580 nm of the light chain region of a 12% sodium dodecyl sulfate acrylamide gel of HMM prepared by a 2-min digestion of myosin with α -chymotrypsin. The gel was stained with Coomassie Blue. The relative areas of the peaks are $LC1:LC2:LC3 = 0.25:0.54:0.21$. The relative amounts of light chains are comparable to that observed in gels of fresh myosin.

viously (3). The extent of labeling was monitored by the percent change in the K^+ EDTA ATPase and Ca^{2+} ATPase activities. The labeled protein was concentrated by ammonium sulfate precipitation or in a Minicon B125 concentrator (Amicon).

^{19}F NMR spectra at 188 MHz were collected on a Nicolet 200 instrument interfaced to a Nicolet 1180 computer. ^{19}F NMR spectra at 254 MHz were collected on a Bruker HX270 instrument interfaced to a Nicolet 1180 computer. Both spectrometers operated in the Fourier Transform mode with quadrature detection. Flat-bottomed 10 mM polished NMR tubes (Wilmad) were used with a nylon vortex suppression plug. Typical sample volumes were between 1 and 1.2 ml. Sweep widths of ± 5000 Hz were used with an acquisition time of 0.409 s. Data size was 8192 points with a pulse delay of 2.0 s, and a typical spectrum included approximately 2000 scans (1.1 h total accumulation time). Chemical shifts were measured relative to *N*-(4-trifluoromethylphenyl)iodoacetamide reacted with dithioerythritol and dissolved in 50% ethanol, 50% D_2O .

The temperature dependence of the NMR chemical shift data was fit assuming a two-state equilibrium between a high temperature (H) and a low temperature (L) species

$$K \\ H \rightleftharpoons L$$

The data were fit with a nonlinear least squares program (20) to the van't Hoff equation

$$-\Delta H_{vh}^{0'} = \frac{\partial (R \ln K)}{\partial (1/T)}$$

The equilibrium constant, *K*, was defined as

$$K = \frac{\delta(T) - \delta_h}{\delta_L - \delta(T)}$$

where δ_h , δ_L , and $\delta(T)$ are the chemical shift of the high temperature species, the low temperature species, and the observed chemical shift at temperature *T*. This procedure defines a van't Hoff enthalpy difference, $\Delta H_{vh}^{0'}$, as opposed to a calorimetrically determined enthalpy difference, $\Delta H_{cal}^{0'}$. $\Delta H_{vh}^{0'} = \Delta H_{cal}^{0'}$ only if the conformational state change is a two-state process (see, for example, Ref. 21). ΔS was calculated from

$$\Delta S = \frac{\Delta H - \Delta G}{T}$$

The estimated error in $\Delta H_{vh}^{0'}$ and $\Delta S^{0'}$ is 10%.

NMR spectra were simulated using an exchange program developed by Kay² or a simulation program provided by Nicolet. It was demonstrated that the rate of exchange had no effect on the derived thermodynamic parameters when the spectral line widths and difference in chemical shift were as observed here.

RESULTS

Fig. 2 shows the ^{19}F NMR spectrum of heavy meromyosin which has been labeled with *N*-(4-trifluoromethylphenyl)iodoacetamide. The conditions of labeling employed here were identical to those used for labeling the SH_1 position of myosin S-1 (3, 6), and the time of the reaction was such that the protein was under-labeled. The Ca^{2+} and K^+ EDTA ATPase activities indicate that 60 (± 10)% of the HMM was labeled (see Ref. 3). As previously seen with S-1- CF_3 , only one resonance is observed in the ^{19}F NMR spectrum of HMM- CF_3 . The line width is approximately 200 Hz (at 188 MHz) at 5 °C.

Fig. 3 is a plot of the ^{19}F chemical shift of the label on HMM as a function of temperature in the absence of divalent metal ion and nucleotide. The data points lie along two curves with the low temperature extreme in chemical shift being approximately 1.45 (± 0.02) ppm, essentially the same as observed for S-1 prepared using either papain or α -chymotrypsin (3, 6). The data fall in the range observed for S-1 and are consistent with the upper temperature extreme observed for

² L. E. Kay, unpublished data.

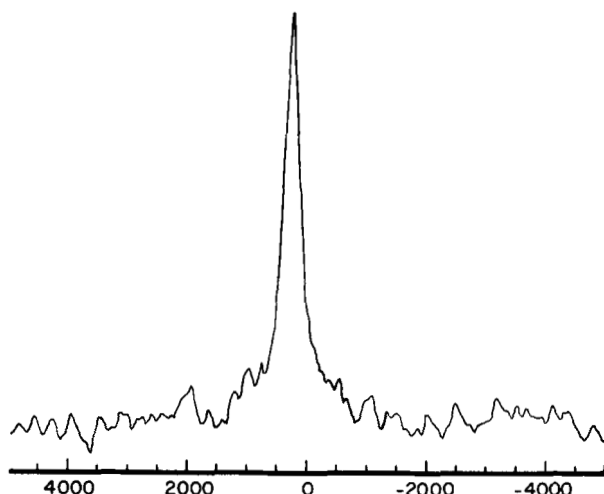


FIG. 2. The ^{19}F NMR spectrum (188 MHz) of HMM- CF_3 . Conditions: 114 μM HMM- CF_3 , 50 mM PIPES, pH 7, 0.1 M KCl, 1 mM EDTA, 10 mM CaCl_2 , 283 K; 2350 transients, 0.409 s acquisition time, 2 s pulse delay, 8192 data points, ± 5000 Hz sweep width.

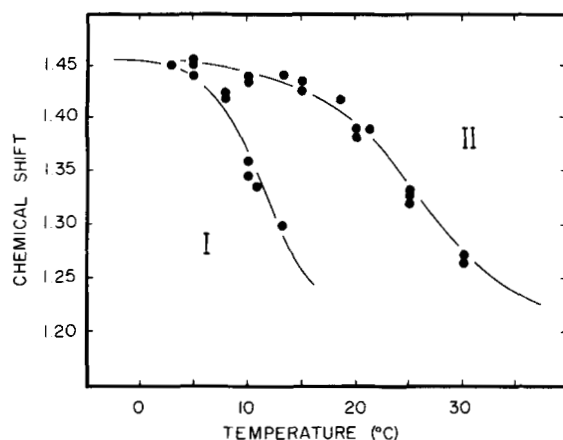


FIG. 3. The ^{19}F NMR chemical shift of HMM- CF_3 in the absence of nucleotide and divalent metal ions as a function of temperature. Conditions were the same as in Fig. 2 except 10 mM EDTA and no $\text{Ca}^{(II)}$ were present. The solid curves are derived from a nonlinear least squares fit. Chemical shifts are in ppm relative to label reacted with dithioerythritol and dissolved in 50% ethanol/50% D_2O at the same temperature (3, 6). Data collected above approximately 15 °C fell on curve II. Decreasing the temperature resulted in data falling on curve I. Data on curve I could be collected if the sample was first cooled to roughly 5 °C and then warmed to the desired temperature.

S-1, i.e. 1.20 (± 0.02) ppm. The data obtained in the absence of divalent metal ions are consistent with two states for the globular heads of HMM which, as far as the ^{19}F NMR probe can detect, are essentially identical to those seen for S-1. Curve II in Fig. 3 can be fit adequately assuming a two-state equilibrium yielding ΔH_{vib}^0 and ΔS^0 values of 41 (± 5) kcal/mol and 147 (± 15) cal/deg/mol, respectively. Curve I can be fit with ΔH_{vib}^0 and ΔS^0 equal to 64 (± 5) kcal/mol and 220 (± 20) cal/deg/mol, respectively.

The two possible curves in Fig. 3 for HMM indicate that under these conditions a hysteresis-like behavior exists, i.e. the observed ^{19}F NMR chemical shift depends on the temperature at which the previous experiment had been performed. A sample equilibrated at low temperature (5 °C) and then monitored at temperatures less than approximately 15 °C yielded a chemical shift which fell on the steeper curve (i.e. curve I). Above roughly 15 °C, the observed chemical shift fell on the less steep curve (i.e. curve II) and subsequent increases

or decreases in temperature resulted in the chemical shift following curve II. Decreasing the temperature from 20 to 10 °C could give data falling on the steeper curve if the sample was kept at 10 °C for sufficient time (e.g. longer than 1 h). Data could only be collected on the steeper curve in the region of 15 °C if the experiments were performed quickly (within 0.5 h) after increasing the temperature from 5 °C. The kinetics of the transition from one path to the other could not be analyzed due to the relatively long time (i.e. 1 h) required to collect spectra of sufficient signal-to-noise ratios.

In Fig. 4 we show the effect of $\text{Ca}^{(II)}$ on the two-state equilibrium of the heads of HMM. The chemical shift extremes are consistent with those seen with S-1, i.e. 1.20 (± 0.02) and 1.45 (± 0.02) ppm, indicating that $\text{Ca}^{(II)}$ does not alter the structure of the heads in the region of SH_1 as far as the ^{19}F probe can determine. The direct observation of the chemical shift of the high temperature state supports our assumption above that chemical shifts characteristic of the two HMM states are identical to the S-1 states. Only one path of interconversion is detected which can be fit assuming a two-state equilibrium with $\Delta H_{\text{vib}}^0 = 65$ (± 5) kcal/mol and $\Delta S^0 = 220$ (± 10) cal/deg/mol. The interconversion is reversible. The presence of $\text{Ca}^{(II)}$ had no noticeable effect on the line width of the ^{19}F resonance.

The effects of $\text{Mg}^{(II)}$ on the equilibrium between the two states of the heads of HMM is shown in Fig. 5. Again the presence of $\text{Mg}^{(II)}$ did not affect the structure of the two states as indicated by essentially the same values for the chemical shift extremes. The data could be adequately fit with the same curve obtained for $\text{Ca}^{(II)}$. $\text{Mg}^{(II)}$ had no apparent effect on the line width of the HMM- CF_3 resonance.

DISCUSSION

The results presented here show that heavy meromyosin, similar to S-1, may be rapidly labeled under mild conditions with *N*-(4-trifluoromethylphenyl)iodoacetamide. The rapidity of the labeling reaction, the activation of the Ca^{2+} ATPase, and inhibition of the K^+ EDTA ATPase indicates that the label reacts preferentially with the so-called SH_1 position similar to that observed for S-1 (3, 6). In the various experiments reported here which perturbed the ^{19}F NMR chemical shift of the probe on HMM, only one resonance was observed, indicating that only one probe site existed. We have obtained no evidence indicating that, under the labeling conditions used here, residues other than the SH_1 are being labeled.

The observed line width of the HMM- CF_3 resonance may

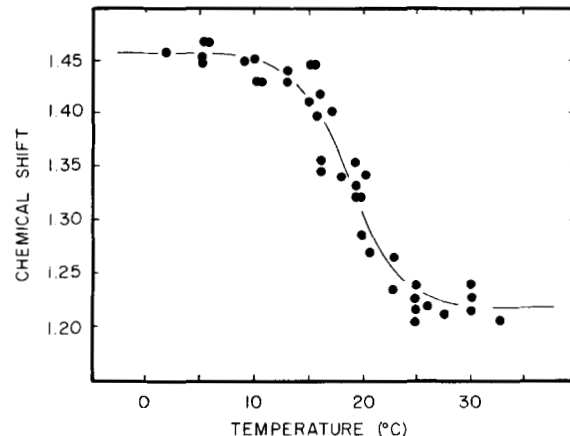


FIG. 4. The ^{19}F NMR chemical shift of HMM- CF_3 as a function of temperature in the presence of $\text{Ca}^{(II)}$. Conditions were the same as in Fig. 2. The solid curve is a nonlinear least squares fit to the data.

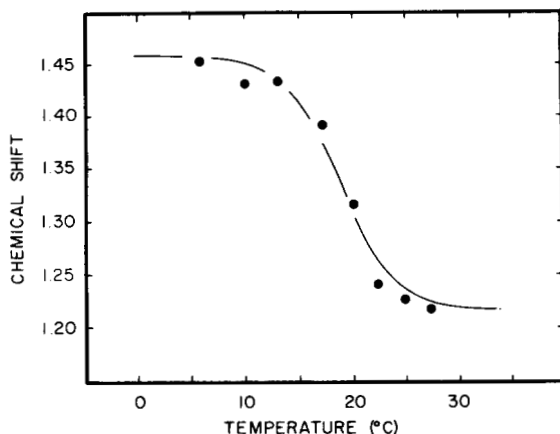


FIG. 5. The ^{19}F NMR chemical shift of HMM- CF_3 as a function of temperature in the presence of $\text{Mg}^{(II)}$. Conditions were the same as in Fig. 2, except for the presence of 2 mM MgCl_2 instead of calcium. The solid curve is the fit derived from the $\text{Ca}^{(II)}$ data in Fig. 4.

be used to calculate a rotational correlation time for the probe assuming that the relaxation is dominated by chemical shift anisotropy (22) and assuming rapid rotation (about the $\text{C-C}(\text{F}_3)$ axis) of the trifluoromethyl group (*i.e.* a rotational correlation time of the trifluoromethyl group of 10^{-11} s). Using the chemical shift tensor elements determined for silver trifluoroacetate (23) we calculate a rotational correlation time for HMM at 5 °C of 3.3×10^{-7} s and 1.7×10^{-7} s at 25 °C. Under similar conditions the rotational correlation time of S-1- CF_3 determined from the ^{19}F line width is 2×10^{-7} s at 5 °C and 1×10^{-7} s at 25 °C. Similar correlation times for S-1 and HMM have been determined using fluorescence depolarization and EPR (24, 25). The temperature dependence of the line width is attributed to the change in viscosity of the solvent. The viscosity of water increases by approximately a factor of 1.8 upon decreasing the temperature from 25 to 5 °C.

The chemical shift of the fluorine probe on HMM is temperature-dependent in a nonlinear manner and lies between two extreme values of 1.20 (± 0.02) and 1.45 (± 0.02) ppm (relative to the free probe reacted with dithioerythritol). These values are taken as indicators of two conformational states of the heads of HMM. The two limiting values are also those seen for S-1 (prepared with either chymotrypsin or papain), which indicates that as far as can be determined from the ^{19}F probe, the two states of the heads of HMM are essentially the same as the two states seen for S-1. A chemical shift between 1.20 and 1.45 ppm apparently results from an equilibrium mixture of the two states. Simulations of NMR spectra assuming two site exchange with line widths of 1 ppm and a line separation of 0.25 ppm show that the exchange rate between the two states could be zero and only a single line would be observed, *i.e.* a lower limit cannot be placed on the exchange rate of the two states. All the experimental data can be adequately fit by assuming two-state equilibria.

The results presented in Fig. 3 indicate that in the absence of divalent metal ions there are two distinct interconversion "paths" between the two HMM states. One path can be fit assuming a two-state equilibrium with $\Delta H_{\text{vh}}^0 = 41 (\pm 5)$ kcal/mol and $\Delta S^0 = 147 (\pm 15)$ cal/deg/mol. These values are similar to those determined for the two-state equilibrium in S-1: $\Delta H_{\text{vh}}^0 = 35 (\pm 5)$ kcal/mol and $\Delta S^0 = 120 (+10)$ cal/deg/mol at pH 7 in PIPES. The other path can be fit assuming a two-state equilibrium with $\Delta H_{\text{vh}}^0 = 64 (\pm 5)$ kcal/mol and $\Delta S^0 = 220 (\pm 20)$ cal/deg/mol and is similar to that obtained upon the addition of Ca^{2+} or Mg^{2+} .

Summarizing all the data collected on S-1 and HMM it would appear that there are basically two types of paths of interconversion between the two states of the globular heads of myosin (Figs. 3-5 in this work and Fig. 5 in (3)) at 0.1 M KCl: the sharper transition is observed only with HMM and characterized by a ΔH_{vh}^0 of approximately 65 kcal/mol and the less steep path is seen with both S-1 and HMM and characterized by ΔH_{vh}^0 of approximately 35-40 kcal/mol. Small differences between examples of each type are observed. For example, the curve in Fig. 4 is shifted to slightly higher temperature than the steeper curve in Fig. 3. In addition the less steep curve in Fig. 3 is shifted relative to that seen for S-1 under similar conditions. These differences can reflect subtle modifications in the cooperative interactions contributing to the two states which are modified, for example, in cleaving the (S-1)-(S-2) hinge when making S-1.

The important observation of this work is the capability of HMM to participate in a two-state transition characterized by ΔH and ΔS values roughly twice those observed for S-1 (Fig. 4). A sharp transition characterized by a ΔH_{vh} on the order of 65 kcal/mol has not been observed for S-1. We give here two possible explanations for these observations which may also explain the hysteresis phenomenon observed for HMM in the presence of EDTA.

It is assumed that the same thermotropic state change observed in S-1 also occurs in the globular heads of HMM. This is supported by the observation of similar limiting chemical shifts for S-1 and HMM, and also that in the presence of EDTA, HMM may behave thermodynamically similar to S-1. The data presented above indicate that there is an additional group of interactions, or possibly a different region or domain, present in HMM that may couple to the region previously observed with experiments on S-1 (3, 6). Coupling of this region to the SH_1 region does not alter the structure of the SH_1 region since essentially the same ^{19}F chemical shifts are observed for the two states in Figs. 3-5. The size, topology, or location of the second region in HMM cannot be specified by the derived thermodynamic parameters. Since the sharper temperature-dependent curve ($\Delta H_{\text{vh}}^0 = 65$ kcal/mol) has not been observed for S-1 under any conditions, the second region is probably external to the S-1 globular head of HMM (although the second region in HMM may be the "second" head, see below).

The additional interactions in HMM may be located in 1) the LC2 light chain, 2) the S-2 segment, or 3) arise from cooperative interactions between the heads. Conformational changes in S-2 and cooperative interactions between the two heads of myosin have been considered in various forms by other workers. The LC2 light chain can be excluded as a site for the additional region in HMM from experiments performed with papain S-1 (6). S-1 prepared with papain contains intact LC2 which is functional in the sense that it binds calcium. This does not exclude a role for the LC2 light chain in coupling the two regions, with the second region being elsewhere in HMM.

Harrington and co-workers (26) have provided evidence for a helix-coil conformational change in the myosin S-2 segment with $\Delta H = 34$ kcal/mol. Harrington has argued that this change may be responsible for contractile force production in muscle (27). If this were true, it would necessarily be coupled to the globular head where the ATPase catalytic site resides.

At present there is little evidence for a cooperative interaction between the heads of rabbit skeletal myosin (28-32). Most of the evidence against a cooperative interaction is from studies involving nucleotides, in contrast to the evidence presented here (25, 33-37). Evidence from experiments with

actomyosin would appear to favor a cooperative interaction between the heads of myosin (38, 39), although in the presence of ATP this may be lost (40).

The additional interactions in HMM may be coupled via the LC2 light chain, which becomes loosely attached at higher temperatures in the absence of metal ion. The hysteresis phenomenon shown in Fig. 3 can be explained if 1) LC2 couples the potentially interacting domains, 2) LC2 dissociates above 15 °C readily in the absence of divalent cations, and 3) recombination of the LC2 is slow and unlikely except at low temperature (e.g. 5 °C). The LC2 light chain may be dissociated from myosin without loss of heavy chain ATPase activity using DTNB or EDTA (19, 41–44). Moss *et al.* (44) have extracted the DTNB light chains from myofibrils using EDTA and elevated temperature. The dissociation of the scallop EDTA light chains (45, 46) and rabbit skeletal light chains (43) is promoted by increased temperature. Wikman-Coffelt *et al.* (43) have previously claimed that re-association of dissociated LC2 occurs more readily at low temperature.

Participation of the LC2 light chain in coupling two regions in HMM is also consistent with the observation that addition of Ca(II) removes the hysteresis effect and only the steeper curve is observed with a $\Delta H_{\text{v}}^{\circ}$ of approximately 65 kcal/mol (Fig. 4). Calcium apparently locks the two regions of HMM into a cooperative unit by binding to the LC2 light chain and stabilizing the light chain-heavy chain interaction. The ΔH value determined from the data in Fig. 3 with Ca(II) is essentially identical to that determined for the steeper curve in Fig. 2 in the presence of EDTA, indicating that Ca(II) basically stabilizes a structure of HMM which was accessible in the absence of Ca(II) at lower temperature.

Mg(II) may also couple the additional regions in HMM. The regions do not appear to uncouple with increase in temperature but behave essentially as seen with Ca(II). Some experiments (not shown) indicated that formation of the larger cooperative unit was not complete within 0.5 h following addition of the Mg²⁺. Kinetic and equilibrium binding data of Robertson *et al.* (16) implies that Mg(II) binds to HMM much more slowly than Ca(II). The Mg(II) on-rate is calculated to be $1.6 \times 10^4 \text{ M}^{-1} \text{ s}^{-1}$ from the binding constant and the measured off-rate. This value is too low for a diffusion-limited binding step. The Ca(II) on-rate is calculated to be $1.4 \times 10^7 \text{ M}^{-1} \text{ s}^{-1}$. These differences may reflect a large difference in a second step following the initial formation of a collision complex which is necessary to form a tight complex.

Divalent metal ions have been shown to stabilize the light chain-heavy chain interaction in rabbit myosin. The most familiar is that proteolysis of the (S-1)-(S-2) hinge region along with the LC2 light chain readily occurs in the absence of divalent cations (47–49). In addition, removal of light chains from rabbit myosin with DTNB or elevated temperature requires the presence of EDTA (14, 44). The metal-binding light chains appear to be more firmly bound to the heavy chains of scallop myosin in the presence of calcium (50).

A cooperative interaction between the two heads of myosin from scallop has been demonstrated (13, 14, 45). The coop-

erative interaction requires the presence of the regulatory EDTA light chains which are similar to the LC2 light chain. Rabbit myosin LC2 light chain may substitute for at least one of the regulatory light chains without loss of Ca²⁺ regulation. Electron micrograph image reconstructions indicate that the regulatory and LC2 light chains extend beyond the (S-1)-(S-2) hinge or “neck” region in myosin (51, 52). The SH₁ region observed in these experiments is located in the 20-kDa fragment which is adjacent to the hinge (52).

REFERENCES

1. Shriver, J. W., and Sykes, B. D. (1981) *Biochemistry* **20**, 2004–2012
2. Shriver, J. W., and Sykes, B. D. (1981) *Biochemistry* **20**, 6357–6362
3. Shriver, J. W., and Sykes, B. D. (1982) *Biochemistry*, **21**, 3022–3028
4. Shriver, J. W. (1984) *Trends Biochem. Sci.* **9**, 322–328
5. Shriver, J. W. (1986) *Biochem. Cell Biol.* **64**, 265–276
6. Tollemar, U., Cunningham, K., and Shriver, J. W. (1986) *Biochim. Biophys. Acta* **873**, 243–251
7. Reisler, E. (1980) *J. Biol. Chem.* **255**, 9541–9544
8. Ebashi, S., and Endo, M. (1968) *Prog. Biophys. Mol. Biol.* **18**, 123–183
9. Weber, A., and Murray, J. M. (1973) *Physiol. Rev.* **53**, 612–673
10. McCubbin, W. D., and Kay, C. M. (1980) *Acc. Chem. Res.* **13**, 185–192
11. Perry, S. V., Cole, H. A., Frearson, N., Moir, A. J. G., Morgan, M., and Pires, E. (1975) in *Molecular Basis of Motility*, 26th Colloquium *Gesellschaft fuer Biologische Chemie* (Heilmeyer, L., ed) pp. 107–121, Springer-Verlag, Heidelberg, Federal Republic of Germany
12. Szent-Györgyi, A. G., Szentkiralyi, E. M., and Kendrick-Jones, J. (1973) *J. Mol. Biol.* **74**, 179–203
13. Chantler, P. D., Sellers, J. R., and Szent-Györgyi, A. G. (1981) *Biochemistry* **20**, 210–216
14. Kendrick-Jones, J., Szentkiralyi, E. M., and Szent-Györgyi, A. G. (1976) *J. Mol. Biol.* **104**, 747–775
15. Bagshaw, C. R., and Reed, G. H. (1977) *FEBS Lett.* **81**, 386–390
16. Robertson, S. P., Johnson, J. D., and Potter, J. D. (1981) *Biophys. J.* **34**, 559–569
17. Lowey, S., Slayter, H. S., Weeds, A. G., and Baker, H. (1969) *J. Mol. Biol.* **42**, 1–29
18. Perry, S. V. (1955) *Methods Enzymol.* **2**, 582–588
19. Wagner, P. (1984) *Biochemistry* **23**, 5950–5956
20. Bevington, P. R. (1969) *Data Reduction and Error Analysis for the Physical Sciences*, McGraw-Hill, New York
21. Lumry, R., Biltonen, R., and Brandts, J. (1966) *Biopolymers* **4**, 917–944
22. Hull, W. E., and Sykes, B. D. (1975) *J. Mol. Biol.* **98**, 121–153
23. Griffin, R. G., Ellett, J. D., Mehring, M., Bullitt, J. G., and Waugh, J. S. (1972) *J. Chem. Phys.* **57**, 2147–2155
24. Thomas, D. D. (1978) *Biophys. J.* **24**, 439–462
25. Mendelson, R. A., Morales, M. F., and Botts, J. (1973) *Biochemistry* **12**, 2250–2255
26. Sutoh, K., Sutoh, K., Karr, T., and Harrington, W. (1978) *J. Mol. Biol.* **126**, 1–22
27. Harrington, W. (1979) *Proc. Natl. Acad. Sci. U. S. A.* **76**, 5066–5070
28. Schaub, M., and Watterson, J. G. (1981) *Biochimie (Paris)* **63**, 291–299
29. Morita, F. (1977) *J. Biochem. (Tokyo)* **81**, 313–320
30. Kodama, T., and Woledge, R. C. (1976) *J. Biol. Chem.* **251**, 7499–7503
31. Kardami, E., de Bruin, S., and Gratzer, W. (1979) *Eur. J. Biochem.* **97**, 547–553
32. Marsh, D. J., d'Albis, A., and Gratzer, W. (1978) *Eur. J. Biochem.* **82**, 219–224
33. Lowey, S., and Luck, S. (1969) *Biochemistry* **8**, 3195–3199
34. Margossian, S., and Lowey, S. (1973) *J. Mol. Biol.* **74**, 313–330
35. Seidel, J., and Gergeley, J. (1973) *Arch. Biochem. Biophys.* **158**, 853–863
36. Mendelson, R. A., and Cheung, P. H. (1976) *Science* **194**, 190–192
37. Taylor, E. (1979) *CRC Crit. Rev. Biochem.* **6**, 103–164
38. Finlayson, B., Lynn, R., and Taylor, E. (1969) *Biochemistry* **8**, 811–819
39. Manuck, B., Seidel, J., and Gergeley, J. (1981) *Biophys. J.* **33**, 233a
40. Fraser, A. B., Eisenberg, E., Kielley, W., and Carlson, F. D. (1975) *Biochemistry* **14**, 2207–2214
41. Gazith, J., Himmelfarb, S., and Harrington, W. F. (1970) *J. Biol. Chem.* **245**, 15–22
42. Weeds, A. G. (1969) *Nature* **223**, 1362–1364
43. Wikman-Coffelt, J., Srivastava, S., and Mason, D. (1979) *Biochimie (Paris)* **61**, 1309–1314
44. Moss, R., Giulian, G., and Greaser, M. (1982) *Biophys. J.* **37**, 365a
45. Kendrick-Jones, J. (1974) *Nature* **249**, 631–634
46. Chantler, P. D., and Szent-Györgyi, A. G. (1980) *J. Mol. Biol.* **138**, 473–492
47. Margossian, S. S., Lowey, S., and Barshop, B. (1975) *Nature* **258**, 163–166
48. Weeds, A. G., and Taylor, R. S. (1975) *Nature* **257**, 54–56
49. Weeds, A. G., and Pope, B. (1977) *J. Mol. Biol.* **111**, 129–157
50. Szent-Györgyi, A. G. (1975) *J. Supramolec. Struct.* **3**, 348–353
51. Vibert, P., and Craig, R. (1982) *J. Mol. Biol.* **157**, 299–319
52. Winkelman, D., Almeda, S., Vibert, P., and Cohen, C. (1984) *Nature* **307**, 758–760